Available online at www.sciencedirect.com
SCIENCE DIRECT®
International Journal of Mass Spectrometry 227 (2003) 439–451
International Journal of Mass Spectrometry
www.elsevier.com/locate/ijms

Structures and fragmentations of zinc(II) complexes of amino acids in the gas phase IV. Solvent effect on the structure of electrosprayed ions

Françoise Rogalewicz, Yannik Hoppilliard, Gilles Ohanessian*

Laboratoire des Mécanismes Réactionnels, UMR 7651 du CNRS, Ecole Polytechnique, 91128 Palaiseau Cedex, France

Received 1 March 2002; accepted 31 July 2002

Abstract

A combination of mass spectrometric and quantum chemical techniques is used to study solvent effects on the structure of desolvated $[AA–H + Zn]^+$ complexes (AA: amino acid), formed in the gas phase by electrospray ionization. By studying the collision-induced fragmentations of such complexes, we show that the solvent used may have a direct impact on the structure of the gaseous ions formed. In the case of $[Gly–H + Zn]^+$, four isomers may be potentially formed, and ions extracted from methanol/water and acetonitrile/water solutions show different fragmentations patterns. The formation of different isomers when using these two solvents is further evidenced by the fragmentation spectra of $[Asn–H + Zn]^+$, and $[Asp–H + Zn]^+$. These cases illustrate the fine tuning which can sometimes be exerted on the structures of electrosprayed ions. Ab initio calculations are used to show the decisive role of the solvent binding energies on the last steps of the electrospray process. It is concluded that both the solvent and the cone voltage in the electrospray source may have a strong influence on the structure of fully desolvated, gaseous ions.

Keywords: Electrospray; Zinc; Amino acids; Solvent effects; Isomerization

1. Introduction

In previous papers of this series [1–3], we have shown that electrosprayed zinc ions must be significantly heated for the last desolvation steps to take place. The energy required for evaporation of the last solvent molecule is high, as in the cases of H_2O and CH_3OH bound to $[Gly–H + Zn]^+$ (binding enthalpies at 298 K of 186 and 218 kJ/mol, respectively). Such energies are large enough that there may exist structural rearrangements with lighter energy demand than final desolvation. In such instances, fully desolvated gaseous ions have a structure which may be different from that of their condensed phase precursors, contrary to what is generally assumed for electrosprayed ions. In fact, a mixture of isomers may be formed. Such isomerizations were shown to occur in the zinc complex of methanol ($[CH_3OZn]^+(CH_3OH)$ isomerizes to $[(CH_2O)(HZn)]^+(CH_3OH)$) and in the zinc complex of the simplest amino acid, glycine: $[Gly–H + Zn]^+(CH_3OH)$, in which three different isomerizations were identified. This work led to the

* Corresponding author. Tel.: +33-1-69-33-35-03; fax: +33-1-69-33-30-41.
E-mail address: gilles@dcmr.polytechnique.fr (G. Ohanessian).

1387-3806/03/$ – see front matter © 2003 Elsevier Science B.V. All rights reserved.
doi:10.1016/S1387-3806(03)00103-9

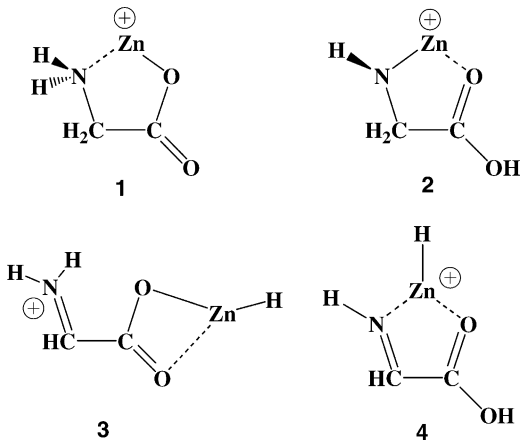

Fig. 1. Isomers of gaseous $[Gly–H + Zn]^+$.

prediction that the solvent may have a direct influence on the desolvation mechanism. This could occur in two different ways: first, stronger ligands to the metal will increase the likelihood of rearrangements being easier than desolvation. Second, protic solvents may act as proton relays between various basic sites of the molecule, opening other pathways for ion isomerization prior to desolvation. The combination of these two effects opens several possible scenarios, depending upon the choice of solvent.

The gas phase complexes of zinc attached to deprotonated amino acids $[AA–H + Zn]^+$ would normally be expected to exist as carboxylate complexes, i.e., deprotonation would occur at the C-terminal carboxylic function which is clearly the most acidic (see **1** on Fig. 1), since this is the probable structure in the parent solution. In a previous paper of this series [2], we have shown that there exist three primary fragmentations for $[Gly–H + Zn]^+$: loss of CO_2, of $H_2O + CO$ and of CO. Loss of $H_2O + CO$ was shown to occur by sequential loss of H_2O first, followed by elimination of CO, therefore the three fragmentations are true parallel pathways. An unexpected result was that **1** cannot give rise to *any* of the observed fragment ions. Indeed, the lowest energy path from **1** is loss of $CO_2 + Zn$ to yield the immonium ion $CH_2NH_2^+$, a fragment that is never observed. This rules out the hypothesis that under collision conditions, **1** would isomerize to some other structure before fragmentation, leading to the conclusion that isomer **1** is never formed in the gas phase. We showed [2] that within the last precursor of $[Gly–H + Zn]^+$, which is mainly [**1**, CH_3OH], transformation into [**3**, CH_3OH] requires less energy than does evaporation of the last "solvent" molecule (see Fig. 1 for non-solvated structures). This isomerization occurs by β-H transfer, a well-known elementary process of organometallic complexes in both gas and solution phases. The new, non-classical structure **3** can itself isomerize into **4** (Fig. 1), either before or after final solvent evaporation. It was shown that **3** and **4** are the precursors for the losses of CO_2 and $H_2O + CO$, respectively.

Finally, loss of CO occurs via isomer **2**, which results from proton transfer from methanol to the carboxylate in Gly, followed by another proton transfer from the amino terminus of Gly to the methoxy group formed by the first proton transfer. Again, formation of [**2**, CH_3OH] from [**1**, CH_3OH] requires less energy than methanol detachment [3]. Desolvation of **2** remains energetically difficult, and a further rearrangement into a four-ligand isomer $[(HOZn)(CH_2NH)(CO)]^+(CH_3OH)$ (labeled CX) is more favorable. From this type of structure, ligand detachment is much easier. These various pathways are summarized in Scheme 1.

The fact that the zinc-solvent binding energy, and the availability of labile protons in the solvent, may influence the formation mechanism of gaseous ions, suggest the intriguing possibility that the structure of a given ion may depend upon the solvent used to prepare the parent solution. For instance, using a non-protic solvent to form gaseous $[Gly–H + Zn]^+$ ions, may prevent formation of isomer **2**. This could be probed by the disappearance of CO loss in the CID spectra of $[Gly–H + Zn]^+$. In the same vein, using a solvent which binds less strongly to zinc than does methanol, may lead to desolvation being less demanding than analyte rearrangement, and therefore lead to the disappearance of the fragmentations described above, to the benefit of immonium formation (loss of CO_2 plus Zn), an ion which can be considered as diagnostic of an acid-deprotonated structure [1,2]. Furthermore,

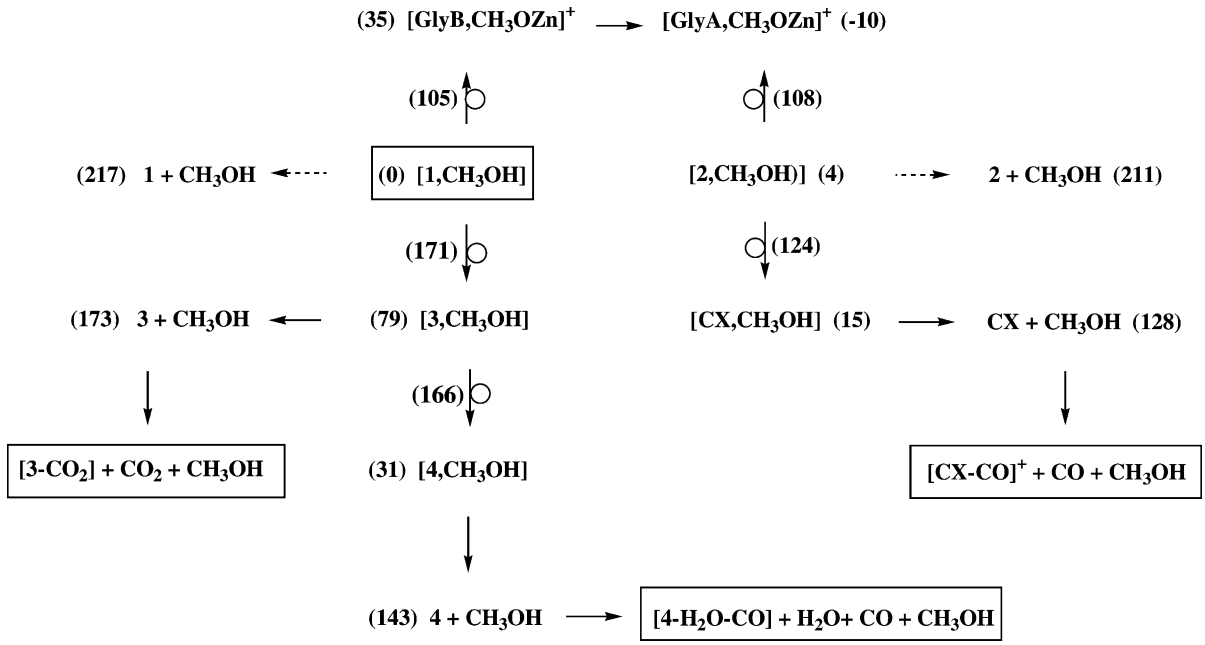

Scheme 1.

it may be anticipated that such processes will occur for the zinc complexes of AA's other than Gly. It is the purpose of this paper to investigate these issues in some detail.

2. Experimental and computational

2.1. Experimental

Electrosprayed zinc complexes of various AA's were formed from an AA/$ZnCl_2$ mixture (500 and 250 μM, respectively) in 50:50 (v/v) solutions of either water/methanol or water/acetonitrile. Such concentrations are typical for the formation of metal complexes of amino acids. In such conditions, the pH is in the 6.5–7 range. Experiments were also tried in pure water or in a 50:50 (v/v) water/pyridine solution, but the resulting spectra could not be exploited for the present study. Solutions were infused in the ion source with a syringe pump (Harvard, Southnatic, MA, USA) at a flow rate of 10 μL/min. Gly, Ser, Thr, Asn, Asp, Gln, His and Met were purchased from Aldrich (Saint Quentin Fallavier, France) and anhydrous $ZnCl_2$ was obtained from Merck KGaA (Darmstadt, Germany). All solvents were of HPLC grade.

All experiments were carried out on a triple quadrupole Quattro II mass spectrometer (Micromass, Manchester, UK). Source parameters were adjusted so as to optimize ion signals (such as $[Gly–H + Zn]^+$). Typical voltage values were: capillary 2.5–3.5 kV, counter electrode 0.1–0.3 kV, RF lens 0.7 eV, skimmer 1.5 V. The cone voltage was varied in the 25–45 V range.

Low-energy collision-induced dissociation (CID) of $[AA–H + Zn]^+$ and their fragments were performed with argon as the collision gas (at a pressure of 6×10^{-4} mbar in the collision cell). The decomposition of $[AA–H + Zn]^+$ was studied as a function of collision energy in the laboratory frame (E_{lab}), typically in the 0–25 eV range. The results will be presented either in the form of individual spectra, or of breakdown graphs showing the abundances of the various fragment ions as a function of collision energy. The gas pressure used

is high enough to allow for multiple collisions, so that the energies imparted to the ions may be higher than the collision energies indicated. All CID experiments were preceded by mass selection of the isotopomer of $[AA–H + Zn]^+$ involving ^{64}Zn.

2.2. Computational

As in our previous work [1–3], two basis sets were used in this study. For geometry optimizations and vibrational frequency calculations, the 6-31G* basis set was used for H, C, N and O, and the Wachters [14s9p5d1f/9s5p3d1f] was used for Zn [4]. This is referred to as basis1. For final energy calculations, basis2 consists in the 6-311+G(2d,2p) for H, C, N and O, and the extended Wachters basis [15s11p6d2f/10s7p4d2f] for Zn. Geometry optimizations and vibrational frequency calculations were carried out at the HF/basis1 level. These calculations were also used to obtain zero point vibrational energies (ZPVE), thermal corrections at 298 K (Etherm) and vibrational entropies in the harmonic approximation. No special treatment was applied to small frequencies. Extensive tests [1–3] showed that the use of HF rather than MP2 geometries leads to very small errors in final energy calculations. Final energetics were obtained with MP2(FC)/basis2 wavefunctions at the HF/basis1 geometries, a level denoted below as MP2(FC)/basis2//HF/basis1 (where FC indicates that the frozen core approximation was applied to the 1s electrons of C, N and O and to the 1s, 2s, and 2p electrons of Zn). The Gaussian 98 program package [5] was used throughout.

3. Results and discussion

3.1. The varying structures of electrosprayed $[Gly–H + Zn]^+$

As recalled above, there are three primary fragmentations of $[Gly–H + Zn]^+$, each of which arises from a specific isomer resulting from a rearrangement prior to desolvation. Among these, loss of CO was shown to arise from a N-deprotonated isomer which is formed within $[Gly–H + Zn]^+(CH_3OH)$ primarily via a double proton transfer mechanism in which the methanol molecule serves as a proton shuttle. The direct consequence of this result is that the use of an aprotic solvent is predicted to shut down the loss of CO channel. Two possibilities may be envisioned: either the solvent is a weak ligand to zinc, and direct desolvation is favored over any rearrangement. In such a case, the non-rearranged structure **1** should be formed, and therefore dominant or exclusive loss of $CO_2 + Zn$ would be predicted. Or else, a strong ligand is used, and rearrangments to **3** and **4** remain more favorable than desolvation. This would lead to two fragmentations of selected $[Gly–H + Zn]^+$: loss of $H_2O + CO$, and loss of CO_2.

Table 1
Binding enthalpies and free energies of possible solvent molecules to $[Gly–H + Zn]^+$, computed at the MP2/b2//HF/b1 level

Solvent	$[Gly–H + Zn]^+$(solvent)	
	ΔH_{298}	ΔG_{298}
H_2O	186	146
CH_2O	191	152
CH_3OH	218	178
HCO_2CH_3	231	190
CH_3COCH_3	255	209
CH_3CN	263	215
C_5H_5N	310	267

All values are given in kJ/mol.

In order to help choose appropriate solvents to check these predictions, ab initio calculations of binding enthalpies and free energies of potential solvent molecules to $[Gly–H + Zn]^+$ were carried out. Since isomer **1** is expected to be the only one present in solution, all calculations involved this isomer. The results are reported in Table 1 and Fig. 2. It may be seen that the seven molecules considered span a wide range of binding enthalpies to zinc in $[Gly–H + Zn]^+$(solvent), from 186 to 310 kJ/mol. These large values cannot be understood solely in terms of the usual electrostatic/polarization interactions. Indeed, they are significantly larger than the corresponding binding energies to sodium [6–8]. The zinc ion is a good electron acceptor, so that significant ligand-to-metal electron transfer also takes place. This may be probed

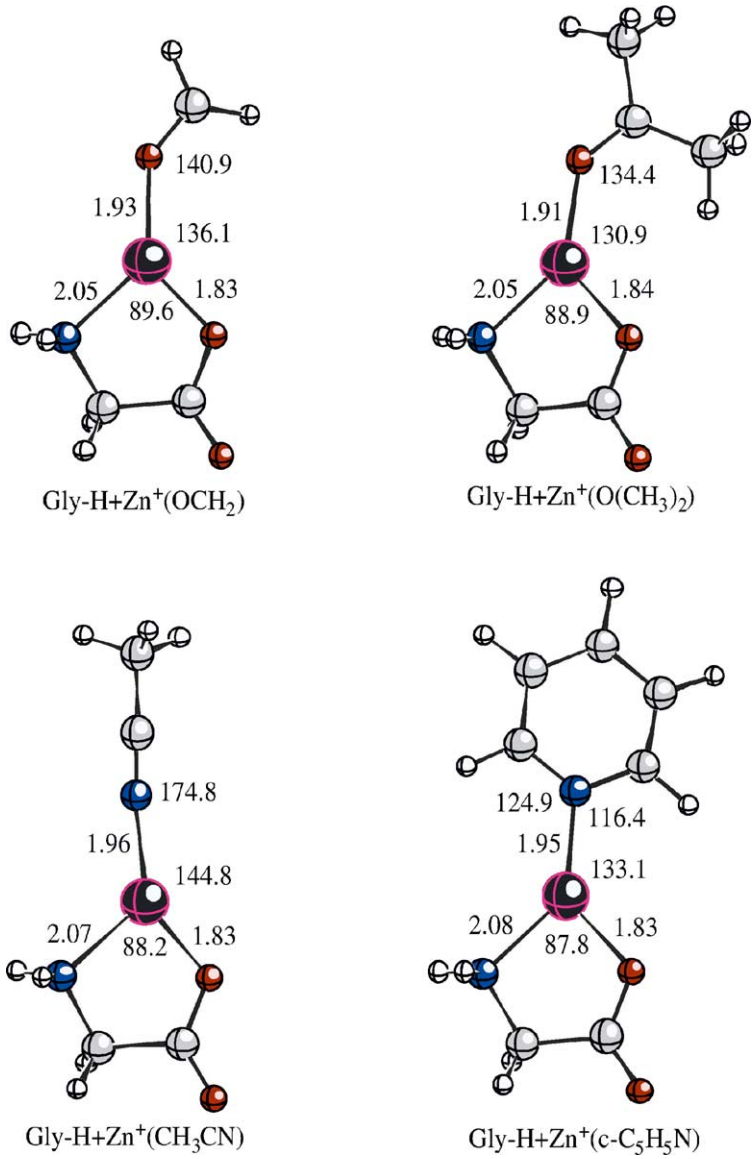

Fig. 2. Optimized structures of $[Gly–H + Zn]^+$(solvent), solvent: methanal, acetone, acetonitrile, pyridine, at the HF/b1 level. Distances in Angstroms, angles in degrees.

by the structure of the complexes with methanal and acetone. The ZnOC angle in $[Gly–H + Zn]^+(OCH_2)$ and $[Gly–H + Zn]^+(O(CH_3)_2)$ shows a strong deviation from 180°, indicating that a vacant metal orbital interacts with a doubly occupied, oxygen lone pair orbital. With a purely electrostatic complex, this angle would be 180° as the metal would favor alignment to the solvent dipole. There is, however, another driving force for non-linearity since the pyridine complex is not symmetric (see Fig. 2). This is likely to be a weak, non-bonded interaction between a solvent C–H bond and the carboxylate O–C bond in Gly. Electron donation to zinc from several sites is competitive, therefore electron donation by a given ligand will be reduced by

an increase in the number of other ligands on the metal, and by an increase of their donation abilities. This reduction of electron donation will be accompanied by a longer metal–ligand bond. The Zn–N and Zn–O bonds to the glycinate are fairly similar in the four complexes shown in Fig. 2 (the Zn–N_{Gly} is only slightly longer in the acetonitrile and pyridine complexes, due to the better donor ability of pyridine compared to methanal and acetone). The difference is more obvious when comparing these structures to that of non-solvated $[Gly–H + Zn]^+$ [1], in which the Zn–N and Zn–O bond lengths are 1.96 and 1.81 Å, respectively.

The two protic solvents, water and methanol, are on the weak ligand side (even though methanol binds strongly enough that direct desolvation is not observed), while polar non-protic solvents have binding enthalpies varying from 191 to 310 kcal/mol. It is expected that methyl formate, acetone, acetonitrile and pyridine, which all bind more strongly to zinc than methanol does, will lead to loss of $H_2O + CO$ and of CO_2, i.e., rearrangements within Gly will take place as with methanol, but loss of CO via structure **2** will not be possible. Methanal, on the other hand, binds less strongly than methanol but by a limited amount (6 kcal/mol), so that it cannot be predicted which of desolvation or rearrangement is more favorable in this case. The binding enthalpies of water and methanal being very close to one another, the favored fragmentation(s) are also difficult to predict in the case of water, with the additional possibility of CO loss induced by water-assisted proton transfer. Thus, these solvents provide, in principle, the possibility of forming gaseous $[Gly–H + Zn]^+$ in several different isomers or mixtures of isomers.

Unfortunately, meaningful spectra could only be obtained in water/methanol and water/acetonitrile solutions. Representative CID spectra of $[Gly–H + Zn]^+$ from both solvents, taken at a collision energy of 12 eV (E_{lab}) are shown in Fig. 3. Breakdown graphs summarizing the CID results as a function of collision energy are shown in Fig. 4. The fragmentation patterns of $[Gly–H + Zn]^+$ arising from the two solvents are clearly different. With the water/methanol solvent and a cone voltage of 35 V (Figs. 3a and 4a), three fragmentations are observed as previously described [3]: loss of $H_2O + CO$ (*m*/*z* 92), loss of CO_2 (*m*/*z* 94), and loss of CO (*m*/*z* 110). With a cone voltage of 45 V, the only significant channel observed in the water/acetonitrile case is loss of CO_2 (Figs. 3c and 4c). While the absence of CO loss was expected (it is actually very weak), that of $H_2O + CO$ loss is more surprising. Complementary information was obtained by using a higher cone voltage in the electrospray source of 45 V in the methanol case (Fig. 3b). Such conditions were expected to favor direct desolvation of [**1**, CH_3OH], however this did not occur as the immonium ion, formation of which is diagnostic of the presence of isomer **1**, was not formed. In fact, the middle spectrum of Fig. 3 and middle graph of Fig. 4 show that in such conditions, the fragmentation pattern of $[Gly–H + Zn]^+$ from the water/methanol solution is very similar to that from the water/acetonitrile solution. This does mean that at higher energies in the desolvation step, rearrangements tend to be disfavored over simple bond cleavages. This shuts down the proton shuttle pathway leading to isomer **2** and eventally to CO loss, and it also disfavors formation of isomer **4** relative to **3**. Indeed, formation of **4** requires an additional rearrangement step from the common [**3**, CH_3OH] intermediate. It is likely that at still higher cone voltages, direct methanol desolvation of [**1**, CH_3OH] would become dominant over rearrangement into [**3**, CH_3OH], but ion intensities are no longer sufficient to probe its occurrence.

3.2. Search for other solvent effects on the structures of electrosprayed $[AA–H + Zn]^+$

CID spectra of $[AA–H + Zn]^+$ (AA = Ser, Thr, Gln, His and Met) were recorded with ions formed from either water/methanol or water/acetonitrile solutions. For Gln, His and Met, no significant difference was found between the fragmentation patterns in both solvents. In such cases, there was no sign of ion rearrangement. For Ser and Thr, the use of water/acetonitrile as the solvent lead to less (Ser) or no (Thr) intensity for the desolvated $[AA–H + Zn]^+$ ion than with water/methanol, as side chain fragmentation becomes the dominant fragmentation pathway.

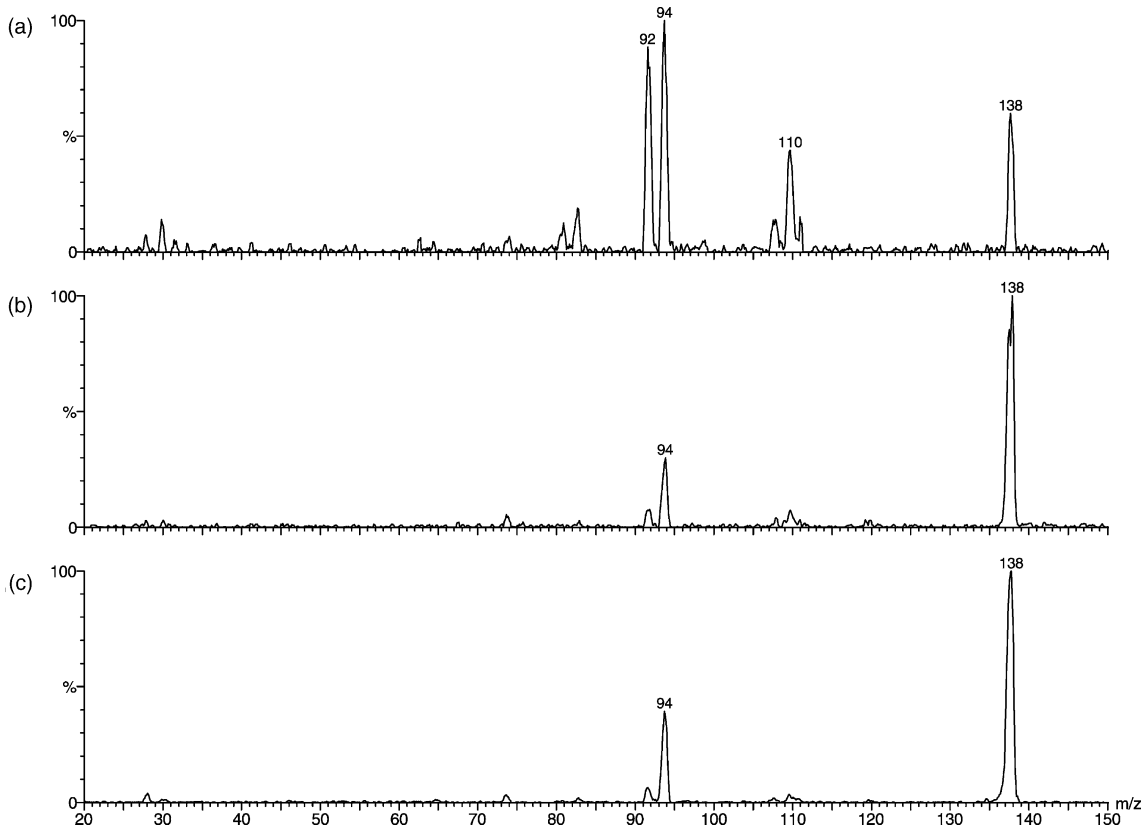

Fig. 3. Fragmentation spectra of $[Gly–H + Zn]^+$ (m/z 138) at 12 eV collision energy in the laboratory frame (E_{lab}). Top: ions generated from a 50:50 (v/v) water/methanol solution with a cone voltage of 35 V. Middle: ions generated from a 50:50 (v/v) water/methanol solution with a cone voltage of 45 V. Bottom: ions generated from a 50:50 (v/v) water/acetonitrile solution with a cone voltage of 45 V.

Although this indicates a solvent influence, it does not necessarily point to different structures being formed in different solvents. All of these studies fall out of the scope of the present paper and will be discussed in a future one.

It is clear that the limited number of solvents leading to efficient formation of $[AA–H + Zn]^+$ provide a small energy window in which to probe fragmentation differences. Since the AA side chain provides an additional attachment site to the metal, the solvent binding energy will vary significantly from one AA to another. It is only when the rearrangement barriers fall in the same range as the methanol and acetonitrile detachment energies that different structures are expected to be formed in the two solvents. Such "favorable" cases turned out to be those of Asp and Asn.

3.3. The varying structures of electrosprayed $[Asp–H + Zn]^+$ and $[Asn–H + Zn]^+$

CID spectra of $[Asp–H + Zn]^+$ formed from a water/methanol and a water/acetonitrile solution are shown in Fig. 5a–c and 5d, respectively. The corresponding breakdown graphs are displayed on the left-hand part of Fig. 6. In the first case, it is seen that for larger values of the cone voltage an intense m/z 88 fragment ion is formed, which corresponds to the immonium ion of Asp with loss of $CO_2 + Zn$. By analogy with the case of $[Gly–H + Zn]^+$ [2], this ion is diagnostic for the formation of the non-rearranged isomer **1**. Also present in Fig. 5 is an m/z 152 fragment ion, corresponding to loss of CO_2, which has been shown to be formed from the rearranged

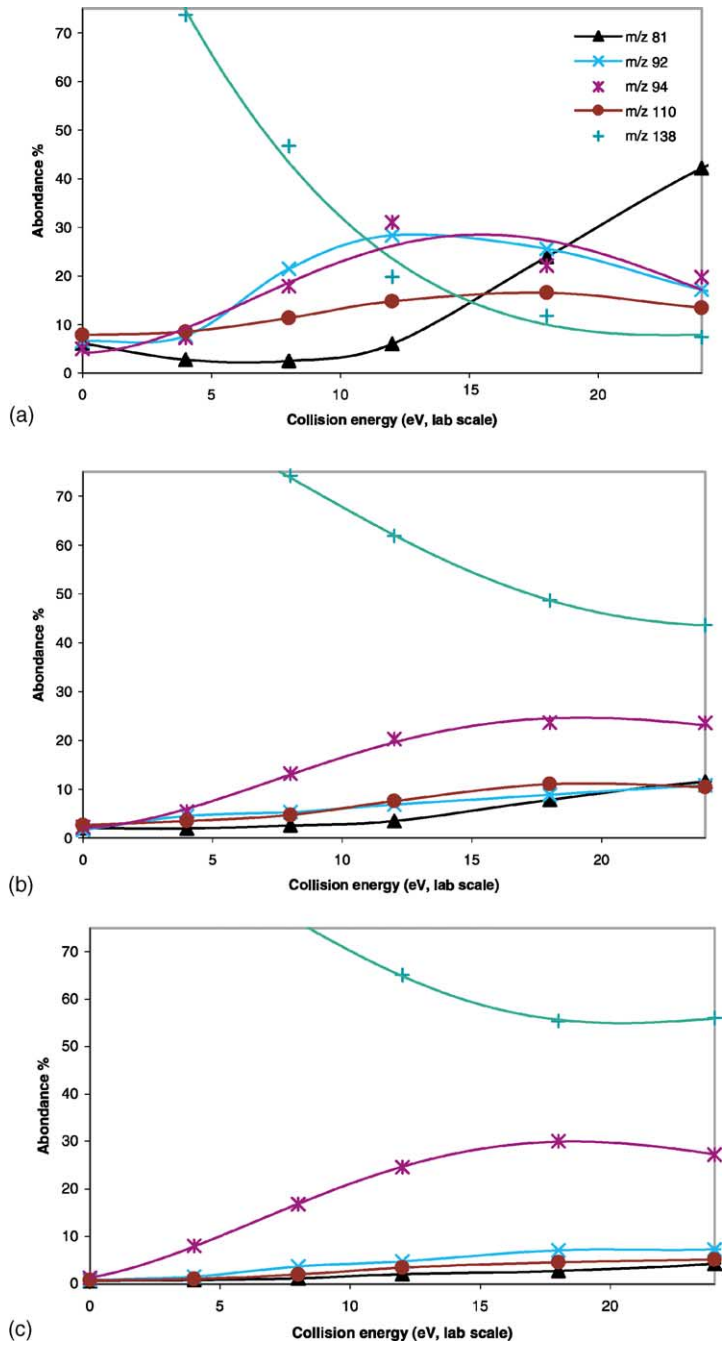

Fig. 4. Breakdown graphs for the fragmentations of $[Gly–H + Zn]^+$ (m/z 138) generated from a 50:50 (v/v) water/methanol solution (a: cone voltage 35 V; b: cone voltage 45 V) and from a 50:50 (v/v) water/acetonitrile solution (c: cone voltage 45 V) as a function of collision energy (E_{lab}).

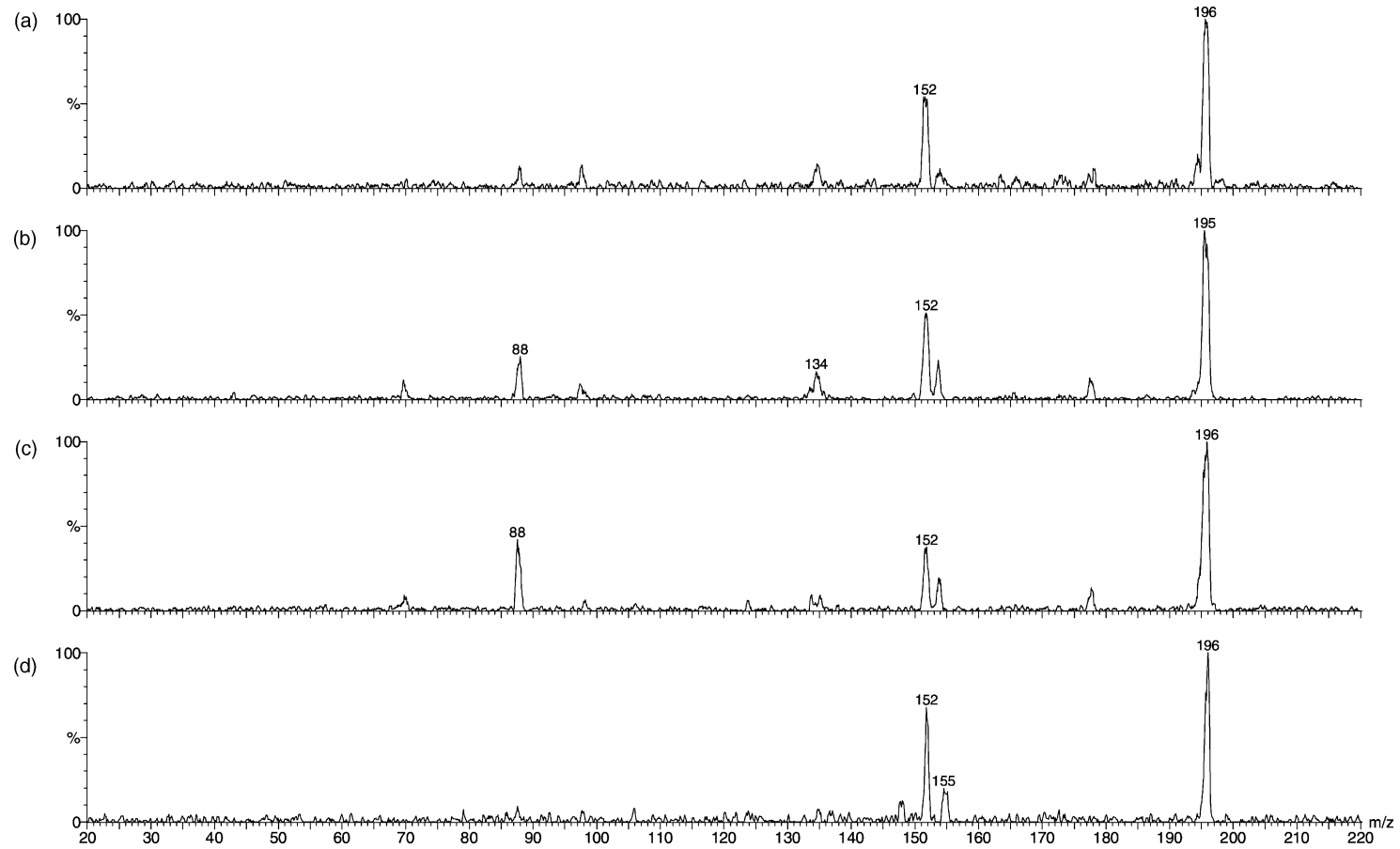

Fig. 5. Fragmentation spectra of $[Asp–H + Zn]^+$ (*m*/*z* 196). (a) Sampling cone voltage 25 V, 50:50 (v/v) water/methanol solution. (b) Sampling cone voltage 35 V, 50:50 (v/v) water/methanol solution. (c) Sampling cone voltage 45 V, 50:50 (v/v) water/methanol solution. (d) Sampling cone voltage 35 V, 50:50 (v/v) water/acetonitrile solution. The peak at *m*/*z* 155 probably corresponds to $(CH_3CN)_2(H_2O)_4H^+$ arising from loss of CH_3CN from *m*/*z* 196 $(CH_3CN)_3(H_2O)_4H^+$.

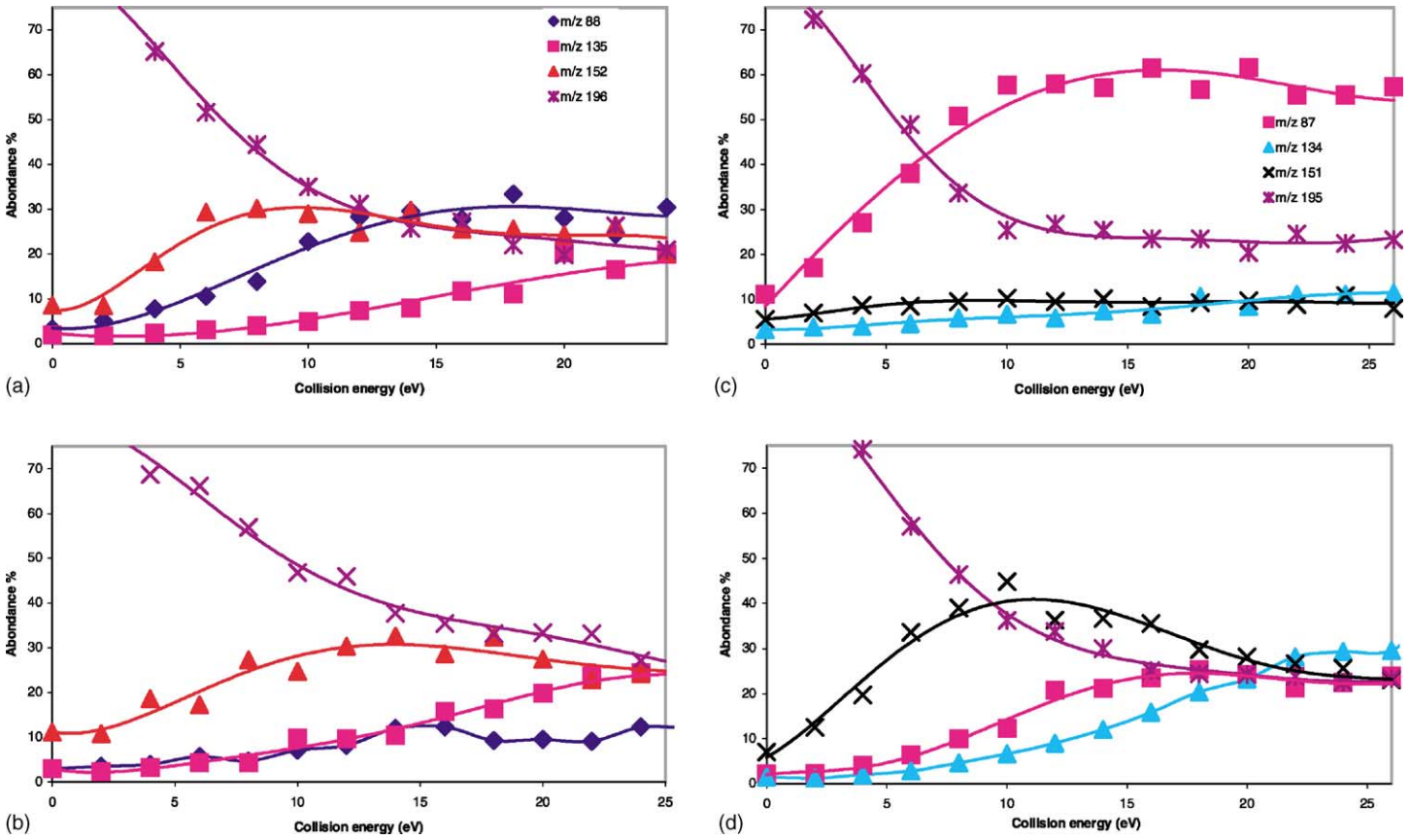

Fig. 6. Breakdown graphs for the fragmentations of ions as a function of collision energy (E_{lab}). (a) $[Asp–H + Zn]^+$ (m/z 196) generated from a 50:50 (v/v) water/methanol solution, and a cone voltage of 30 V; (b) $[Asp–H + Zn]^+$ (m/z 196) generated from a 50:50 (v/v) water/acetonitrile solution, and a cone voltage of 30 V; (c) $[Asn–H + Zn]^+$ (m/z 195) generated from a 50:50 (v/v) water/methanol solution, and a cone voltage of 25 V; (d) $[Asn–H + Zn]^+$ (m/z 195) generated from a 50:50 (v/v) water/acetonitrile solution, and a cone voltage of 35 V.

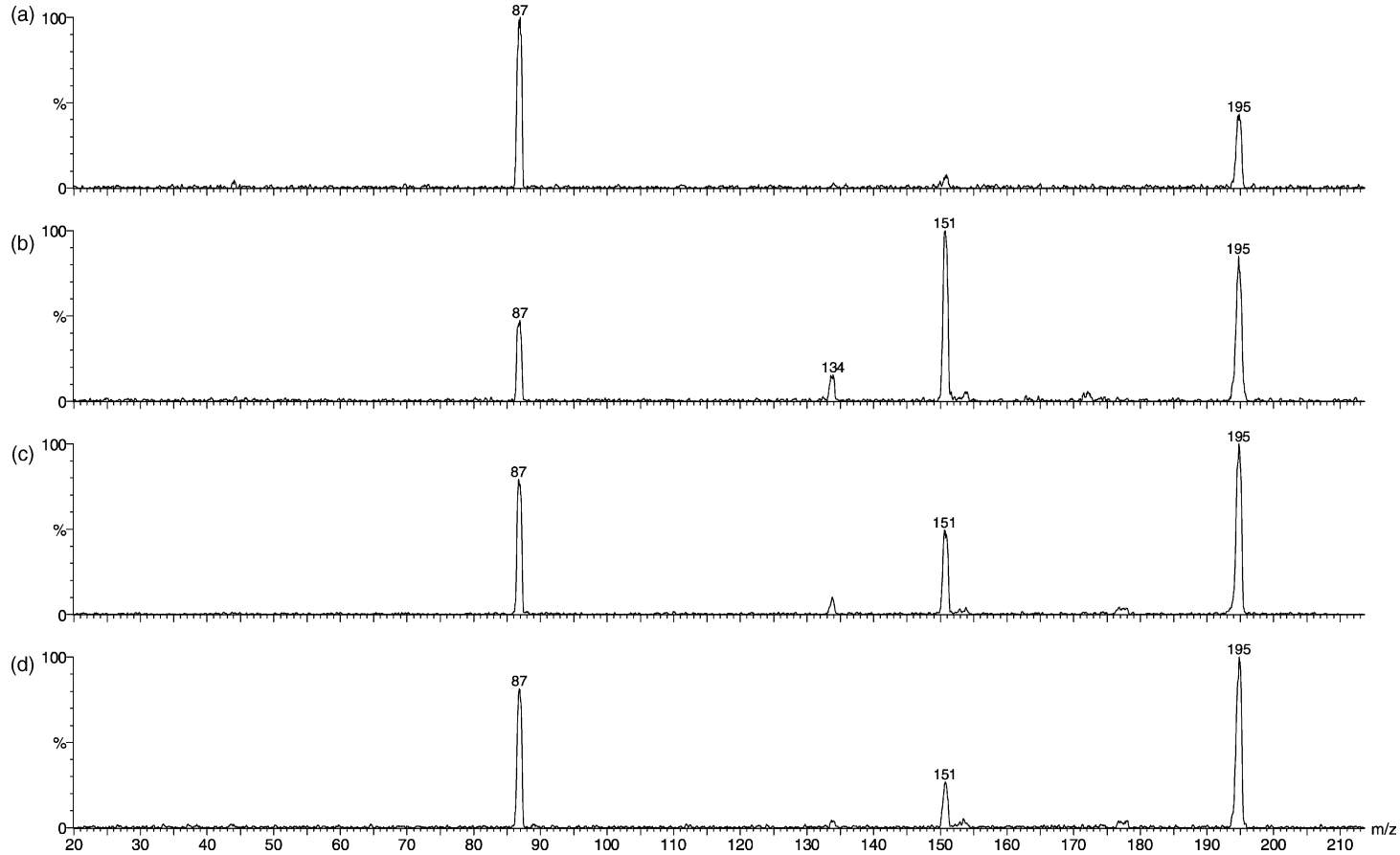

Fig. 7. Fragmentation spectra of $[Asn–H + Zn]^+$ (*m/z* 195). (a) Sampling cone voltage 35 V, 50:50 (v/v) water/methanol solution. (b) Sampling cone voltage 25 V, 50:50 (v/v) water/acetonitrile solution. (c) Sampling cone voltage 35 V, 50:50 (v/v) water/acetonitrile solution. (d) Sampling cone voltage 45 V, 50:50 (v/v) water/acetonitrile solution.

Table 2
Binding enthalpies and free energies of methanol and acetonitrile molecules to a series of $[AA–H + Zn]^+$ complexes, computed at the MP2/b2//HF/b1 level

Species	CH_3OH		CH_3CN	
	ΔH_{298}	ΔG_{298}	ΔH_{298}	ΔG_{298}
$[Asn–H + Zn]^+$	169	132	210	176
$[Asp–H + Zn]^+$	197	159	238	203
$[Gly–H + Zn]^+$	218	178	263	215

All values are given in kJ/mol.

isomer **3**. When the solvent used is water/acetonitrile, the latter is the only significant fragment ion except for a *m/z* 155 ion, see legend of Fig. 5. These results may be interpreted by a competition between desolvation and rearrangement when methanol is bound to $[Asp–H + Zn]^+$, while in the case of acetonitrile, direct desolvation of **1** can no longer compete efficiently with rearrangement because of the higher desolvation energy with acetonitrile than with methanol. The quantum chemical results in Table 2 indicate that the acetonitrile binding enthalpy to $[Asp–H + Zn]^+$ is indeed larger than that of methanol by 41 kJ/mol. It may also be seen that both values are smaller than their Gly analogues, explaining why direct desolvation of methanol can compete with rearrangement in the case of Asp but not in the case of Gly.

The interpretation of the $[Asp–H + Zn]^+$ results is corroborated by those obtained for $[Asn–H + Zn]^+$. As seen in Table 2, the binding enthalpies of CH_3OH and CH_3CN are smaller to $[Asn–H + Zn]^+$ than they are to $[Asp–H + Zn]^+$. As shown in Fig. 8, the structures of solvated $[Asp–H + Zn]^+$ and $[Asn–H + Zn]^+$ involve a distorted tetrahedral environment around the metal, since side chain folding provides an additional binding site as compared to glycine analogues shown in Fig. 2. The third ligand is the side chain carbonyl oxygen in Asp, while it is the amide nitrogen in Asn. Since the latter is a better electron donor, it weakens the binding energy of the solvent molecule to the metal more efficiently. As a consequence, desolvation of any given molecule is expected to require less energy from $[Asn–H + Zn]^+$ than from $[Asp–H + Zn]^+$.

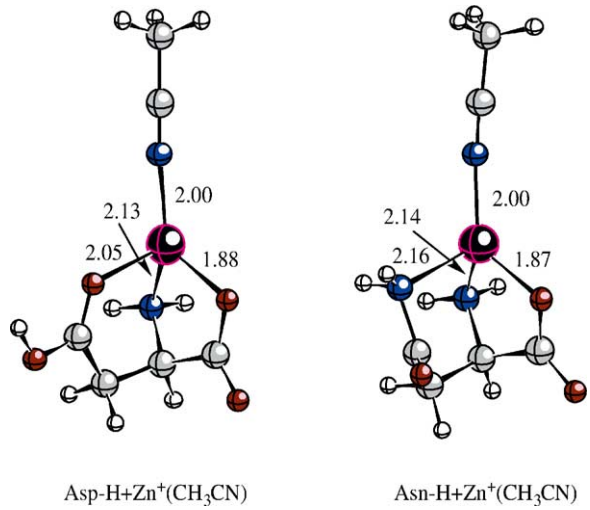

Fig. 8. Optimized structures of $[AA–H + Zn]^+$(acetonitrile), AA: Asp and Asn, at the HF/b1 level. Distances in Angstroms, angles in degrees.

With methanol, the binding enthalpy drops down to 169 kJ/mol, to be compared to 197 and 238 kJ/mol for $[Asp–H + Zn]^+$ and $[Gly–H + Zn]^+$, respectively. The CID spectrum shown in Fig. 7a and the breakdown graph shown in the upper right part of Fig. 6 show that, in agreement with these values, the only significant low-energy fragmentation of $[Asn–H + Zn]^+$ formed from a water/methanol solution is loss of $CO_2 + Zn$ (*m/z* 87), corresponding to direct desolvation to isomer **1**. When the water/acetonitrile solvent is used, the higher binding enthalpy of CH_3CN (210 kJ/mol vs. 169 kJ/mol for methanol) re-opens the rearrangement pathway. Indeed, at low cone voltage (see Fig. 7b), the dominant dissociation mode becomes CO_2 loss (*m/z* 151) and loss of $CO_2 + Zn$ is much less intense. At higher cone voltages (Fig. 7c and d), simple bond breaking is favored over isomerization, and loss of $CO_2 + Zn$ becomes dominant again. The higher the cone voltage, the higher the internal energy of the desolvating ions, and the more favored is direct solvent evaporation.

Comparison of the fragmentations of $[Asp–H + Zn]^+$ and $[Asn–H + Zn]^+$ from both solvents illustrates the influence of desolvation energy on

the structure of fully desolvated ions. When desolvation and rearrangement have similar critical energies, as appears to be the case here, fine tuning of the solvent binding energy leads to switching between the two processes. Lowering this energy favors solvent evaporation; this is achieved either by using methanol instead of acetonitrile, or by considering Asn instead of Asp with a given solvent.

4. Conclusions

Electrospray formation of $[AA–H + Zn]^+$ may lead to several different structures, via rearrangment of AA–H within $[AA–H + Zn]^+$(solvent), prior to the last desolvation step. This has been shown in the case of $[Gly–H + Zn]^+$, for which fragmentation spectra differ between ions formed from water/methanol and water/acetonitrile solutions. The difference is attributable to the larger energy require to desolvate $[Gly–H + Zn]^+$ from acetonitrile. This is shown by the fragmentation differences with the water/methanol solvent when the electrospray cone voltage is varied. Higher energies in the electrospray region eventually favor direct bond breaking (here, desolvation) over rearrangements. Solvent-dependent structures have also been established for electrosprayed $[Asp–H + Zn]^+$ and $[Asn–H + Zn]^+$; moreover, the fragmentation patterns of these two closely related AA's are distinctly different, and these differences can be interpreted in terms of solvent binding energies. It is concluded that whenever the last desolvation step and analyte rearrangement have similar critical energies, the choice of solvent and source cone voltage may have a strong influence on the structure of gaseous, electrosprayed ions.

Acknowledgements

We thank Gilles Louazel for carrying out the calculations on Asp and Glu complexes. This work was supported by a grant of computer time at the Institut de Développement et de Ressources en Informatique Scientifique (IDRIS, project 010543).

References

[1] F. Rogalewicz, Y. Hoppilliard, G. Ohanessian, Int. J. Mass Spectrom. 201 (2000) 307.
[2] F. Rogalewicz, Y. Hoppilliard, G. Ohanessian, Int. J. Mass Spectrom. 204 (2001) 267.
[3] F. Rogalewicz, Y. Hoppilliard, G. Ohanessian, Int. J. Mass Spectrom. 206 (2001) 45.
[4] (a) A.J.H. Wachters, J. Chem. Phys. 52 (1970) 1033;
(b) P.J. Hay, J. Chem. Phys. 66 (1977) 4377.
[5] M.J. Frisch, G.W. Trucks, H.B. Schlegel, G.E. Scuseria, M.A. Robb, J.R. Cheeseman, V.G. Zakrzewski, J.A. Montgomery Jr., R.E. Stratmann, J.C. Burant, S. Dapprich, J.M. Millam, A.D. Daniels, K.N. Kudin, M.C. Strain, O. Farkas, J. Tomasi, V. Barone, M. Cossi, R. Cammi, B. Mennucci, C. Pomelli, C. Adamo, S. Clifford, J. Ochterski, G.A. Petersson, P.Y. Ayala, Q. Cui, K. Morokuma, D.K. Malick, A.D. Rabuck, K. Raghavachari, J.B. Foresman, J. Cioslowski, J.V. Ortiz, B.B. Stefanov, G. Liu, A. Liashenko, P. Piskorz, I. Komaromi, R. Gomperts, R.L. Martin, D.J. Fox, T. Keith, M.A. Al-Laham, C.Y. Peng, A. Nanayakkara, C. Gonzalez, M. Challacombe, P.M.W. Gill, B. Johnson, W. Chen, M.W. Wong, J.L. Andres, C. Gonzalez, M. Head-Gordon, E.S. Replogle, J.A. Pople, Gaussian 98 (Revision A.6), Gaussian Inc., Pittsburgh, PA, 1998.
[6] S. Hoyau, K. Norrman, T.B. McMahon, G. Ohanessian, J. Am. Chem. Soc. 121 (1999) 8864.
[7] T.B. McMahon, G. Ohanessian, Chem. Eur. J. 6 (2000) 2931.
[8] M.T. Rodgers, P.B. Armentrout, Mass Spectrom. Rev. 19 (2000) 215.